HHS Public Access

Author manuscript

Environ Pollut. Author manuscript; available in PMC 2021 June 01.

Published in final edited form as:

Environ Pollut. 2020 June ; 261: 114183. doi:10.1016/j.envpol.2020.114183.

Prebiotic inulin consumption reduces dioxin-like PCB 126-mediated hepatotoxicity and gut dysbiosis in hyperlipidemic Ldlr deficient mice

Jessie B. Hoffman[1,2], **Michael C. Petriello**[1,3,4,#], **Andrew J Morris**[1,3,4], **M. Abdul Mottaleb**[1,3,4], **Yipeng Sui**[2], **Changcheng Zhou**[2,##], **Pan Deng**[1,5], **Chunyan Wang**[1,5], **Bernhard Hennig**[1,5,*]

[1]Superfund Research Center, University of Kentucky, Lexington, KY, USA

[2]Department of Pharmacology and Nutritional Sciences, College of Medicine, University of Kentucky, USA

[3]Division of Cardiovascular Medicine, College of Medicine, University of Kentucky, Lexington, KY, USA

[4]Lexington Veterans Affairs Medical Center, Lexington, KY, USA

[5]Department of Animal and Food Sciences, College of Agriculture, Food and Environment, University of Kentucky, Lexington, KY, USA

Abstract

Exposure to some environmental pollutants increases the risk of developing inflammatory disorders such as steatosis and cardiometabolic diseases. Diets high in fermentable fibers such as inulin can modulate the gut microbiota and lessen the severity of pro-inflammatory diseases, especially in individuals with elevated circulating cholesterol. Thus, we aimed to test the hypothesis that hyperlipidemic mice fed a diet enriched with 8% inulin would be protected from

[*]Correspondence should be directed to: Bernhard Hennig, 900 S. Limestone Street, Superfund Research Center, University of Kentucky, Lexington, KY 40536, USA. Tel.: +1 859-218-1343; fax: +1 859-257-1811; bhennig@uky.edu.

[#]Current address: Institute of Environmental Health Sciences and Department of Pharmacology, Wayne State University, Detroit, MI, USA

[##]Current address: Division of Biomedical Sciences, School of Medicine, University of California, Riverside, CA, USA

CRediT author statement

Jessie B. Hoffman: Conceptualization, Methodology, Investigation, Writing - Original Draft
Michael C. Petriello: Investigation, Methodology, Funding acquisition
Andrew J Morris: Resources, Funding acquisition
M. Abdul Mottaleb: Investigation
Yipeng Sui: Investigation
Changcheng Zhou: Supervision, Funding acquisition
Pan Deng: Investigation, Visualization, Writing - Review & Editing
Chunyan Wang: Investigation
Bernhard Hennig: Supervision, Writing - Review & Editing, Funding acquisition

Declaration of interests

The authors declare that they have no known competing financial interests or personal relationships that could have appeared to influence the work reported in this paper.

the pro-inflammatory toxic effects of PCB 126. Four groups of male *Ldlr*$^{-/-}$ mice were fed a high cholesterol diet containing 8% inulin or 8% cellulose (control) for 12 weeks. At weeks 2 and 4, mice were exposed to PCB 126 or vehicle (control). PCB 126 exposure induced wasting and impaired glucose tolerance, which were attenuated by inulin consumption. PCB 126 exposure induced hepatic lipid accumulation and increased inflammatory gene expression, which were both decreased by inulin consumption. In addition, inulin feeding decreased atherosclerotic lesion development in the aortic root and modulated the expression of enzymes related to glycolysis. Finally, 16S rRNA sequencing of gut microbial populations showed that PCB 126 modulated multiple microbiota genera (e.g., 3-fold decrease in *Allobaculum* and 3-fold increase in *Coprococcus*) which were normalized in inulin fed mice. Overall our data support the hypothesis that a dietary intervention that targets the gut microbiota may be an effective means of attenuating dioxin-like pollutant-mediated diseases.

Main finding: Dietary inulin protected against PCB 126 induced inflammation, atherosclerosis, and dysbiosis.

Graphical Abstract

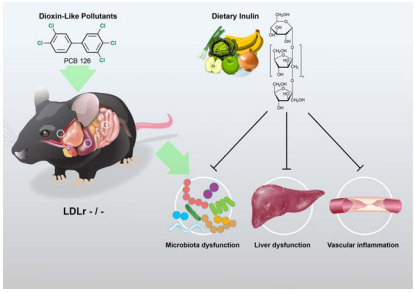

Keywords

dioxin; gut microbiota; polychlorinated biphenyls; fiber; inulin

Introduction

Exposure to dioxin-like pollutants poses numerous health risks including increased risk of cardiometabolic diseases such as diabetes, steatosis and atherosclerosis (Carpenter, 2006; World Health Organization, 2016). Due to the lipophilic nature of dioxin-like pollutants, humans are primarily exposed through consumption of contaminated fatty foods such as fish, beef, and dairy products (Carpenter, 2006; Perkins et al., 2016). Importantly, this route of exposure allows for the possibility of the gastrointestinal tract and associated gut microbiota to come into contact with high levels of dioxin-like pollutants and therefore makes it a critical target organ to study. The gut and gut microbiota play an important role in overall host health and disruptions of these systems have been implicated in the development of several diseases including cardiometabolic and hepatic diseases (Barko et al., 2018). Our laboratory has previously demonstrated that exposure to the dioxin-like pollutant PCB 126 increases intestinal inflammation, disrupts gut microbiota, and alters host metabolism, and can accelerate development of cardiometabolic diseases (Petriello, 2018; Petriello et al., 2018). Because of these findings demonstrating the toxicity of PCBs on the gut microbiota

and gut health, utilization of dietary interventions to attenuate or mitigate these negative effects may be a simple and readily feasible means of reducing disease risks associated with dioxin-like pollutant exposure.

Prebiotics are “a selectively fermented ingredient that allows specific changes both in the consumption and/or activity in the gastrointestinal microbiota that confers benefits upon host well-being and health” (Robles Alonso and Guarner, 2013). The most widely understood and accepted prebiotics include certain types of dietary fiber (Clemens et al., 2012). However, not all fibers are prebiotic. Fibers that have been documented to have functional prebiotic properties include fructooligosaccharides, galactooligosaccharides, some disaccharides, some nonstarch polysaccharides, and inulin (Florowska et al., 2016). Conversely, insoluble fibers such as cellulose, are minimally fermented by the gut microbiota and thus exhibit little prebiotic activity. The prebiotic nature of fibers come, in part, from the structural bonds and the ability of the gut microbiota to enzymatically metabolize these bonds (Flint et al., 2012). The human gastrointestinal tract is colonized by little to no cellulolytic bacteria, therefore cellulose passes through the gastrointestinal tract minimally fermented (Flint et al., 2012). In contrast, many bacteria inhabiting the human gastrointestinal tract have been observed to possess enzymes capable of breaking the structural linkages found in fructans (Flint et al., 2012). The prebiotic inulin is a fructan that contains linear chains of fructosyl groups linked by β(2–1) glycosydic bonds, terminated with an α-D(1–2)-glucopyranoside ring group on the reducing end (Mensink et al., 2015). Inulin is a potent prebiotic that has been demonstrated clinically to promote gut microbiota that have been associated with good health, including *Bifidobacterium* spp, and *Lactobacillus* spp (Vandeputte et al., 2017). Aside from modulation of the gut microbiota, consumption of inulin can reduce adiposity and improve glucose sensitivity (Dewulf et al., 2011; Salazar et al., 2015). Furthermore, inulin administration has recently been shown to protect against hepatic steatosis through multiple mechanisms (Chambers et al., 2018; Sugatani et al., 2012; Sugatani et al., 2006). Importantly, a meta-analysis found that the most notable effect of consumption of inulin-type fructans was on lowering of low density lipoprotein (LDL) levels, an effect well-evidenced to lower the risk of adverse cardiovascular events. Thus, the objective of this study was to elucidate the role of prebiotic nutritional intervention (i.e. inulin) on attenuating PCB-induced disruption of hepatic, cardiometabolic, and gut microbiota health.

Materials and Methods

Animals, diets, and study design

Seven-week-old male *Ldlr*−/− mice were purchased from Jackson Laboratories and maintained on a 12-h light/ 12-h dark cycle at a temperature of 22°C with 50% humidity. All mice received food and water *ad libitum* and measures of food intake and body weight were recorded weekly. The base diet for this study has been previously shown to cause hyperlipidemia in *Ldlr* deficient mice and the dosing schedule and concentration has previously been shown to produce circulating parts per billion levels of PCB 126 (Petriello et al., 2018). Following one week of acclimation, mice were randomly divided into 4 groups (n=10). Mice were fed either a control high cholesterol diet containing 8% cellulose as the

fiber source (2 groups; n=10 each) or a prebiotic containing high cholesterol diet with 8% of inulin as the fiber source (2 groups; n=10 each). Inulin and cellulose were incorporated directly into the formulation of the purified diets (Research Diets Inc., New Brunswick, NJ). The level of fiber in this study was chosen to represent a “high” fiber intake based on human dietary recommendations. The recommended intake of fiber is 14g per 1000 calories (Agriculture, 2015). The established level of fiber in purified rodent diets is 5%, equating to 12g per 1000 calories. The 8% level of fiber equates to 21g per 1000 calories, which can be classified as a “high” fiber diet. Detailed diet compositions can be found in Supplemental Table 1. At weeks 2 and 4, mice received either 1 μmol/kg of PCB 126 (AccuStandard, CT, USA) or safflower oil vehicle (Dyets, Bethlehem, PA, USA) via oral gavage. This dosing schedule has been previously used by our lab and produces plasma levels of PCB 126 that mimic human exposure levels to dioxin-like pollutants (Petriello, 2018; Petriello et al., 2018) At the end of the study mice were fasted for 16 h, anesthetized and blood was collected via retro-orbital bleed. Liver and cecum samples were collected, snap frozen in liquid nitrogen, and stored at −80°C until analysis. All experimental procedures were approved by the Institutional Animal Care and Use Committee of University of Kentucky.

Glucose tolerance testing and body composition analysis

Intraperitoneal GTTs were conducted on weeks 5 and 8 based on our previous study which revealed PCB-induced trends towards glucose intolerance at week 5 and loss of these trends by week 12 (Petriello, 2018). The inclusion of an earlier timepoint (week 8) was done in an attempt to better capture any trends that were missing from our first study. Mice were fasted for 6 h and given an IP injection of glucose (i.e. 20% solution at 2 mg/g BW, sterile saline). Blood from the tail vein was collected at baseline, 15, 30, 60, 90, and 120 minutes post injection and blood glucose levels were quantified using a hand-held glucometer (Accu-check Avivia, Roche, Basel, Switzerland). Lean body mass and fat mass were analyzed at week 10 using EchoMRI (EchoMRI LLC, Houston, TX, USA).

DNA Extraction and 16S rRNA Sequencing

DNA extraction and 16S rRNA gene sequencing (V4–V5 region) were conducted by the Environmental Sample Preparation and Sequencing Facility (ESPSF) at Argonne National Laboratory as previously discussed in detail (Petriello, 2018), and following procedures described by Caporaso et. al (Caporaso et al., 2012). Analysis was conducted using the program Quantitative Insights into Microbial Ecology (QIIME version 1.9) by Argonne National Laboratories. Specifically, reads were joined using the “join_paired_ends.py” command followed by “split_libraries_fastq.py” to demultiplex using the default parameter of 1.5 mismatches. *De novo* operational taxonomic units (OTUs) were then picked using the command “pick_de_novo_otus.py” and any observations present less than twice were filtered from the OTU table prior to statistical analysis. The sequencing data were deposited in the ArrayExpress database.

Hepatic histology

Sections of liver were fixed in 10% neutral buffered formalin and subsequently embedded in paraffin for histological examinations. Hepatic tissues sections were stained with hematoxylin-eosin (H&E) and examined by a pathologist usinglight microscopy and visually

scored for macrovesicular or microvesicular fat. Photomicrographic images were captured at 20x magnification using a Nikon Eclipse (Melville, NY) 55iUpright microscope attached to a 12MP color camera.

RNA Extraction and qPCR

Liver samples were homogenized in TRIzol (Invitrogen, Carlsbad, CA) and mRNA was extracted according to manufacturer's instructions. Quality and concentrations were quantitated using a NanoDrop 2000 spectrophotometer (Thermo Scientific, Waltham, MA) as conducted in previous studies (Petriello, 2018; Petriello et al., 2018; Wahlang et al., 2017a). Complimentary DNA was generated utilizing qScript cDNA SuperMix with genomic DNA wipeout (Quantabio, Beverly, MA). Gene expression was determined via qPCR utilizing Taqman fast reagents (Thermo Scientific, Waltham, MA) in a CFX96 Real-Time PCR system (Bio-Rad, Hercules, CA). The Taqman primers used were *Tnfa* (Mm00443258_m1), *Lbp* (Mm00493139_m1), *Tlr4* (Mm00445273_m1), *Mrp2* (Mm00445273_m1), *Pklr* (Mm00443090_m1), *Gck* (Mm00439129_m1), *Pck1* (Mm00439129_m1), *G6pc* (Mm00839363_m1) *18S* was used as the housekeeping gene after determination that expression values varied fairly tightly in line with *Actb* measures and based on previous validated use in a similar animal model (Petriello et al., 2016). The ΔΔCt relative quantification method was used to calculate fold differences in gene expression.

Quantitation of atherosclerotic lesions

To quantify extent of atherosclerosis, aortic roots were frozen in OCT, sectioned at 10 μm per section, and stained with oil red O as before (Petriello et al., 2018). Briefly, serial sections were collected as close as possible to the observance of the three valves and sections were placed on microscope slides (Probe-on Plus; Fisher Scientific, Pittsburgh, PA) until the aortic valves disappeared. Frozen sections were stained with oil red O and images were taken using a Nikon Eclipse 55iUpright microscope attached to a 12 MP color camera. Subsequent images were quantified for lesion area by Image-Pro Software Plus 4.5.

PCB quantification in liver and plasma

PCB 126 was extracted and analyzed by GC-MS/MS. Briefly, samples were homogenized, extracted in 1:1 volume of deionized water and acetonitrile (1% acetic acid) and transferred to an Agilent Bond Elut QuEChERS fatty sample dispersive 2 ml SPE column. PCB 126 was analyzed using an Agilent GC-triple quadrupole MS (GC-MS/MS) 7000C system equipped with a multimode inlet and a HP-5MS UI column (30m, 0.25mm, 0.25um) in multiple reaction monitoring (MRM) mode. Ion transitions monitored were 325.9/255.9 for PCB 126 and 337.9/267.9 for 13C12-PCB 126 internal standard. Relative quantitation was done by comparing peak area of the sample to peak area of an internal standard sample of known concentration.

Albumin protein quantification in plasma

Mouse albumin levels were determined by ELISA using a commercially available kit as per the company's instructions (Abcam, ab108791). Samples were normalized for protein concentration using the BCA Assay.

Statistical analyses

Data were analyzed using GraphPad PRISM or SigmaPlot 14 and are presented as mean ± SEM. Comparisons between groups were made by two-way ANOVA with post-hoc comparisons of the means. Statistical significance was set at a determined p value of $p<0.05$.

Results

Inulin consumption and PCB exposure exert differential effects on body composition

Overall, inulin fed mice of both groups gained less body weight from the beginning of the study and cellulose fed mice exposed to PCBs gained significantly greater weight than PCB-exposed mice fed inulin (5.92 g vs 4.07 g; p=0.010). (Suppl. Figure 1A). EchoMRI measurements of body composition revealed that PCB exposure resulted in wasting as determined by reductions in percent body fat in cellulose fed mice, but this was not observed in inulin fed mice (Suppl. Figure 1B). Importantly, there were no differences in food intake between all the groups (Suppl. Figure 1C).

Inulin reduces PCB-induced hepatic steatosis

When examining liver composition, we observed that PCB 126 exposure significantly increased liver weight in cellulose fed mice, which was attenuated with inulin consumption (Figure 1A). Overall, inulin-fed mice exhibited lower liver weights compared to cellulose fed mice and a significant overall effect of PCB exposure on increasing liver weights was apparent. Vehicle exposed mice within the control cellulose diet exhibited apparent macrovesicular fat accumulation due to the high cholesterol diet and this fatty infiltration was drastically abolished due to inulin feeding. As observed previously, PCB 126 exposure resulted in microvesicular fatty change, which was also less abundant in inulin fed mice as determined by a clinical pathologist (Figure 1B).

Inulin attenuates PCB-induced hepatic inflammation and alters markers of xenobiotic metabolism

PCB 126 exposure drastically increased (~10 fold) hepatic expression of tumor necrosis factor alpha (*Tnfa*) which was completely attenuated by inulin consumption (Figure 1C). Furthermore, PCB 126 increased expression of an additional marker of inflammation, Lipopolysaccharide binding protein (*Lbp*) in cellulose but not inulin-fed mice. Additionally, Inulin fed mice irrespective of treatment exhibited reduced levels of pro-inflammatory toll like receptor 4 (*Tlr4).* Furthermore, exposed inulin fed mice exhibited lower levels of multidrug resistance protein (*Mrp2*) compared to exposed cellulose-fed mice (Figure 1C).

Inulin protects against PCB 126 disruption of glucose tolerance.

To assess the effects of pollutant exposure and inulin consumption on glucose tolerance, an intraperitoneal glucose tolerance test (IPGTT) was conducted at weeks 5 and weeks 8. At week 5, PCB 126-exposure increased fasting blood glucose levels (~1.16 fold in cellulose fed mice and such an increase was not observed in inulin-fed mice (Figure 2A). Overall, mice fed inulin displayed increased glucose sensitivity ($p<0.0001$). Furthermore, cellulose fed mice exposed to PCBs displayed significantly decrease glucose sensitivity (i.e., a greater area under the curve (AUC)) compared to PCB exposed mice fed inulin. At week 8 (6 weeks after the first PCB 126 dose), no significant differences in fasting blood glucose were observed, but the effects of PCB exposure and inulin feeding on AUC observed at week 5 remained similar (Figure 2B). No differences in circulating insulin, GLP-1, or c-peptide levels at the end of the study were observed (data not shown).

Inulin and PCBs differentially alter hepatic markers of glucose metabolism.

To elucidate the effects of PCB exposure and inulin consumption on glucose metabolism, hepatic expression of key glycolytic and/or gluconeogenic enzymes was examined (Figure 3). PCB exposure significantly reduced expression of pyruvate kinase (*Pklr*) in cellulose fed mice, while the reduction in exposed inulin fed mice was not significant. Additionally, an overall reductive effect of PCB exposure on glucokinase (*Gck*) and phosphoenolpyruvate carboxykinase (*Pck1*) expression was observed, regardless of diet. However, an overall effect of inulin consumption on increasing *Pck1* expression was observed. Furthermore, glucose 6-phosphatase (*G6pc*) expression was significantly increased in inulin fed mice, regardless of exposure.

Inulin feeding decreases atherosclerotic lesion formation

We quantified atherosclerotic lesion areas within the aortic roots using Oil Red-O staining and determined that overall, inulin fed mice displayed significantly decreased lesion formation compared with cellulose fed mice ($p=0.012$) (Figure 4A). Also, it was determined that PCB treated mice fed inulin displayed significantly decreased lesion formation than PCB treated mice fed the control cellulose diet (Mean Cellulose+PCB; $1.75\times10^5 \pm 6.93\times10^4$ μm^2, Mean Inulin+PCB; $1.19\times10^5 \pm 4.68\times10^4$ μm^2, $p<0.05$; Figure 4B–C). An overall effect of PCB exposure was not observed.

Inulin feeding does not modulate circulating levels of PCB 126

In an attempt to possibly explain the observed protection due to inulin throughout this study, we hypothesized that fiber intake may decrease circulating levels of the lipophilic PCB 126. Therefore, using GC-MS/MS we quantitated PCB 126 in plasma and livers at the conclusion of the study. It was determined that 8% inulin feeding had no impact on circulating PCB 126 concentrations (Mean Cellulose+PCB; 3.98 pg/μL; Mean Inulin+ PCB; 4.13 pg/μL, $p=0.90$) (Figure 5A). Unexpectedly however, Inulin consumption increased hepatic levels of PCB 126 (Mean Cellulose+PCB; 2020.09 pg/mg tissue ± 338.47 pg/mg tissue; Mean Inulin +PCB; 3008.99 pg/mg tissue ± 870.26 pg/mg tissue, $p=0.045$) (Figure 5A). In an attempt to explain the increased PCB 126 levels within the liver we quantified albumin levels by ELISA; albumin is known to bind persistent organic pollutants such as PCBs. We

determined that overall, inulin significantly increases hepatic albumin levels (Figure 5B). Post-hoc analysis determined that mice fed inulin and exposed to PCB 126 exhibited ~2-fold increase in albumin protein compared with exposed mice fed cellulose as the fiber source. Finally, we correlated hepatic PCB 126 concentrations with hepatic albumin and observed a nearly significant modest association (r^2= 0.37; p=0.062) (Figure 5C).

Inulin and PCB 126 exert differential effects on gut microbial populations

Upon examination of gut microbial populations via 16S rRNA sequencing, we observed several significant main effects and interactions between pollutant exposure and inulin consumption. At the phylum level, mice fed inulin had lower levels of Verrucomicrobia than cellulose fed mice, irrespective of exposure (1.53 fold-difference, p<0.0001) (Table 1). Furthermore, a significant increase (40.5-fold difference, p<0.0001) in Actinobacteria was observed due to inulin feeding. Additionally, a significant increase in Bacteroidetes was apparent in vehicle treated inulin fed mice compared to vehicle treated cellulose fed mice (2.73-fold difference, p<0.0001). There were no significant effects of pollutant exposure on the Firmicutes to Bacteroidetes ratio, however a significant diet effect was observed in which inulin fed mice had a lower ratio than cellulose fed mice (Suppl. Figure 2A). Alpha diversity, as calculated using the Shannon Diversity Index, revealed a significant exposure effect with PCB exposed mice having a reduced diversity compared to non-exposed mice, but this was not altered by inulin feeding (Suppl. Figure 2B).

At the genera level, a significant increase in *Coprococcus* in cellulose fed mice exposed to PCB 126 was found (3.06-fold difference, p=0.0088), which was attenuated by inulin feeding (Table 1). PCB exposed mice fed the cellulose diet also exhibited a trend towards reductions in *Allobaculum* which was significantly increased by inulin feeding. Furthermore, inulin exposure significantly increased the abundance of *Bifidobacterium* (56-fold difference, p<0.0001) and *Lactobacillus* (16.9-fold difference, p<0.0001) and reduced the abundance of *Ruminococcus* (1.79-fold difference; p<0.0001). Inulin fed mice also exhibited lower levels of *Akkermansia*, irrespective of pollutant exposure (1.53-fold difference, p<0.0001).

Discussion

Exposure to environmental pollutants, specifically dioxin-like pollutants, poses numerous health threats to those exposed, including metabolic disruptions, hepatic lipid accumulation, and gut dysbiosis. A common route of exposure to dioxin-like pollutants is through contaminated foods and thus the gastrointestinal system is exposed to the highest amounts of these pollutants. Utilizing a mouse model of cardiometabolic disease, our lab has previously demonstrated that exposure to PCB 126 induces gut dysbiosis, increases systemic and intestinal inflammation, accelerates atherosclerosis, and also induces metabolic dysfunction (Petriello, 2018; Petriello et al., 2018). It is well understood that nutritional modulation of pollutant toxicity is an effective means of reducing detrimental health effects of pollutant exposure (Hennig et al., 2012). Therefore, in this study we sought to examine the role of prebiotic nutritional intervention (i.e., a diet enriched with the fermentable fiber inulin) on attenuating our previous observations of PCB-induced disruption of gut microbiota and

cardiometabolic health. Our data demonstrate that inulin feeding can attenuate PCB-induced disruption of gut microbiota, host metabolism, hepatic steatosis, and inflammation.

The gastrointestinal tract is a key organ that is tightly linked to various organ systems including the liver, cardiovascular system, and sympathetic nervous system (Baskin et al., 2014; Moos et al., 2016; Tripathi et al., 2018). The gut microbiota, defined as the trillions of bacteria residing within the gastrointestinal tract can be strongly influenced by dietary and environmental factors and may play a role in the detrimental health effects observed with PCB exposure, as well as during nutritional interventions. For example, mice fed inulin had a lower Firmicutes/Bacteroidetes ratio, irrespective of exposure. This may suggest a "healthier" microbial composition in our inulin mice, since the Firmicutes/Bacteroidetes ratio is increased in chronic inflammatory diseases and metabolic syndrome.

When looking at more specific microbial populations, interesting effects of both diet and exposure were apparent. For this study, we utilized 16s rRNA gene sequencing to elucidate the changed in microbial populations from the taxonomic level of phylum to the level of genus. Attribution at the species level is not recognized as valid for accurate interpretations, so we did not include this taxonomic level in our analysis (Johnson et al., 2019). When examining microbial populations in this study, the levels of *Akkermansia*/Verrucomicrobia observed in our study were notably elevated in all groups, compared to a typical murine microbial signature (Lagkouvardos et al., 2016). This observation was previously noted by our group, and we hypothesize that the high levels of cholesterol in this model are influencing the growth of these bacteria (Petriello, 2018). *Akkermansia muciniphila* is commonly recognized as a beneficial bacterium, consuming intestinal mucin and enhancing barrier function (Derrien et al., 2004). However, researchers have noted that an overabundance of *A. muciniphila* can actually exacerbate intestinal inflammation in mice (Ganesh et al., 2013). Our observation of strikingly elevated levels of *Akkermansia*/Verrucomicrobia in this high cholesterol model is a very important finding that should be pursued further to better elucidate the specific mechanisms driving the large bloom of these bacteria.

The genus *Allobaculum* appears to be sensitive to dietary interventions. A significant diet effect of inulin increasing the level of this genus, irrespective of exposure was observed. It has been demonstrated that *Allobaculum* decreases under high fat feeding and that prebiotic (oligofructose) feeding is able to increase the abundance of this genera (Everard et al., 2014). This increase with prebiotic treatment has been reproduced several times in the scientific literature (Everard et al., 2014; Tachon et al., 2013; Van Hul et al., 2018). Importantly, the genus *Allobaculum* has been associated with improved intestinal barrier function and also resistance to the development of NAFLD (Le Roy et al., 2013). Additionally, increases in *Allobaculum* have also been observed with metformin treatment, a clinically effective drug used for the management of diabetes (Zhang et al., 2015). Therefore, our findings of increased *Allobaculum* abundance in all groups fed inulin may be associated with our findings of reduced hepatic steatosis/inflammation and improved glucose tolerance and metabolism.

In addition to the gastrointestinal tract, dioxin-like pollutants are known to exert various effects throughout the body; one such effect being induction of significant loss of body weight, known as wasting (Mandal, 2005). PCB exposure resulted in a significant reduction in body fat percentage, while inulin-fed mice were protected from this effect. Interestingly, throughout the study, inulin fed mice gained less weight than cellulose fed mice, highlighting the potential adipose specific wasting induced by toxicant exposure only observed in cellulose fed mice. Our group has previously observed this wasting effect upon exposure to PCB 126 in a mouse model of non-alcoholic steatohepatitis (NASH) (Wahlang et al., 2017b), indicating that liver injury may play a role in this wasting effect.

When examining systemic host health, the liver is of utmost importance. The liver is a vital organ responsible for metabolism of both dietary constituents and pollutants and is the second organ, following the gut, that comes in contact with polychlorinated biphenyls. In individuals with gut dysbiosis and/or cardiovascular disease, it is common to observe liver pathologies such as nonalcoholic steatohepatitis (NASH) or nonalcoholic fatty liver disease (NAFLD) (Baskin et al., 2014; Tripathi et al., 2018). Importantly, it is well accepted that exposure to persistent organic pollutants contributes to the pathogenesis of NASH and NAFLD and thus has been recognized as its own entity, “toxicant induced steatohepatitis” (TASH) (Wahlang et al., 2013). We have recently shown that exposure to PCB 126 can drastically exacerbate NADLS-like liver and metabolic dysfunction induced by feeding a methionine-choline deficient (MCD) diet, resulting in wasting, increased systemic inflammatory markers, and presence of hepatic fibrosis (Wahlang et al., 2017b).

Hepatic macrovesicular fat accumulation is what is most commonly observed in obesity and NASH/NAFLD and is characterized by lipid droplets that accumulate extrahepatocellularly. Macrovesicular lipid accumulation was apparent in unexposed cellulose fed mice, consistent with our previous studies and the progression of cardiometabolic disease that is induced using the present mouse model. However, in cellulose fed mice exposed to PCB 126, a shift from macrovesicular to microvesicular lipid accumulation was observed, indicating a disruption in energy metabolism and/or lipid transport. Importantly inulin fed mice were protected from both macrovesicular and microvesicular hepatic lipid accumulation. This reduction in hepatic lipid accumulation with inulin feeding is consistent across numerous studies (Chambers et al., 2018; Javadi et al., 2018; Mistry et al., 2018; Sugatani et al., 2006). Importantly, in humans, it was observed that inulin and inulin-propionate ester supplementation attenuate hepatic steatosis in patients with NAFLD (Chambers et al., 2018). To our knowledge, the present study is the first to examine inulin supplementation on dioxin-like pollutant exposure, but inulin feeding has been studied in context of other xenobiotics. For example, it was demonstrated that inulin supplementation reduced hepatic steatosis and xenobiotic-induced (i.e. phenobarbital) liver injury in rats fed a high fat, high sucrose diet (Sugatani et al., 2006). One mechanism by which inulin may attenuate hepatic steatosis is hypothesized to be through the production of short chain fatty acids, specifically propionate (Sugatani et al., 2012).

Inflammation is a driver in many chronic diseases, especially that of hepatic inflammation. The attenuation of PCB induced increases in expression of *Tnfa* and *Lbp* by inulin feeding may be due to the reduction in hepatic lipid accumulation and/or microbial-driven

interactions. Interestingly, in vehicle treated mice, inulin feeding resulted in a significantly elevated expression of Lbp. We hypothesize that this finding may be due to elevated levels of specific microbial taxa due to the drastic difference in fermentability of inulin compared to cellulose. For example, Knapp et al., found that Lbp is essential to the innate immune response to *Eschericia coli* in peritonitis (Knapp et al., 2003). Nevertheless, this unexpected finding deserves further examination in subsequent studies.

Due to the liver being the central hub of metabolic processes, it is well understood that hepatic inflammation and lipid accumulation can alter overall metabolism, especially glucose metabolism (Hazlehurst et al., 2016; Keramida et al., 2016). In the present study, PCB exposure in cellulose fed mice resulted in glucose intolerance at both weeks 5 and 8 of the study, as evidenced by an increased area under the curve. Importantly, inulin feeding was able to attenuate these disruptions in glucose tolerance. PCB impairment in glucose tolerance has also been documented by others (Baker et al., 2013; Jensen et al., 2014). To better understand the mechanisms behind these improvements in glucose tolerance observed with inulin feeding, gene expression of hepatic enzymes involved in glycolysis and gluconeogenesis were quantified. Examining the rate limiting enzymes of glycolysis revealed that PCB exposure significantly reduced pyruvate kinase (*Pklr*) and phosphofructokinase (*Pfkl*) gene expression in mice fed cellulose, but not in mice fed inulin. There was also an insignificant decrease in glucokinase (*Gck*) expression in cellulose fed mice, which was not present in inulin fed mice. To our knowledge, these PCB-induced alterations in hepatic glycolytic enzymes have not been reported previously and could play a role in an inability to properly metabolize glucose. We hypothesize that these alterations were attenuated in inulin fed mice due to our observed improvements in hepatic lipid accumulation and inflammation, as these factors have been demonstrated to contribute to metabolic dysfunction (Hazlehurst et al., 2016; Keramida et al., 2016).

Conclusion

Overall, the data presented demonstrate that consumption of the prebiotic inulin is capable of attenuating PCB 126-induced disruption of gut microbial population, host metabolism and inflammation. It does not appear that inulin was effective at decreasing the body burden of PCB 126, thus the observed protection may be related to the production of protective metabolites, decreases in atherogenic lipoproteins and cholesterol, or other unknown mechanisms that can be examined in future studies. We hypothesize that through alterations in gut microbial populations and microbial metabolite production, that inulin is able to reduce cardiometabolic disease risk. Future studies will need to examine if the formation of short chain fatty acids or other microbiota-dependent metabolites are critical mediators of our observed protection by dietary inulin against PCB-mediated hepatotoxicity.

Supplementary Material

Refer to Web version on PubMed Central for supplementary material.

Acknowledgement

The authors would like to acknowledge Dr. Eun Lee for histological evaluations. We thank Tom Dolan (Medical Illustration, College of Medicine, University of Kentucky) for preparing the figure for the Graphical Abstract.

Funding: This work was supported by the National Institute of Environmental Health Sciences, National Institutes of Health [P42ES007380; K99ES028734; R00ES028734; R01ES023470; R01HL131925] and the University of Kentucky Agricultural Experiment Station. The content is solely the responsibility of the authors and does not necessarily represent the official views of the National Institutes of Health.

Reference

Agriculture, U.S.D.o.H.a.H.S.a.U.S.D.o., 2015 2015–2020 Dietary Guidelines for Americans., 8th Edition ed.

Baker NA, Karounos M, English V, Fang J, Wei Y, Stromberg A, Sunkara M, Morris AJ, Swanson HI, Cassis LA, 2013 Coplanar polychlorinated biphenyls impair glucose homeostasis in lean C57BL/6 mice and mitigate beneficial effects of weight loss on glucose homeostasis in obese mice. Environ Health Perspect 121, 105–110. [PubMed: 23099484]

Barko PC, McMichael MA, Swanson KS, Williams DA, 2018 The Gastrointestinal Microbiome: A Review. J Vet Intern Med 32, 9–25. [PubMed: 29171095]

Baskin KK, Bookout AL, Olson EN, 2014 The heart-liver metabolic axis: defective communication exacerbates disease. EMBO Mol Med 6, 436–438. [PubMed: 24623378]

Caporaso JG, Lauber CL, Walters WA, Berg-Lyons D, Huntley J, Fierer N, Owens SM, Betley J, Fraser L, Bauer M, Gormley N, Gilbert JA, Smith G, Knight R, 2012 Ultra-high-throughput microbial community analysis on the Illumina HiSeq and MiSeq platforms. ISME J 6, 1621–1624. [PubMed: 22402401]

Carpenter DO, 2006 Polychlorinated biphenyls (PCBs): routes of exposure and effects on human health. Rev Environ Health 21, 1–23. [PubMed: 16700427]

Chambers ES, Byrne CS, Rugyendo A, Morrison DJ, Preston T, Tedford C, Bell JD, Thomas L, Akbar AN, Riddell NE, Sharma R, Thursz MR, Manousou P, Frost G, 2018 The effects of dietary supplementation with inulin and inulin-propionate ester on hepatic steatosis in adults with non-alcoholic fatty liver disease. Diabetes Obes Metab.

Clemens R, Kranz S, Mobley AR, Nicklas TA, Raimondi MP, Rodriguez JC, Slavin JL, Warshaw H, 2012 Filling America's fiber intake gap: summary of a roundtable to probe realistic solutions with a focus on grain-based foods. J Nutr 142, 1390S–1401S. [PubMed: 22649260]

Derrien M, Vaughan EE, Plugge CM, de Vos WM, 2004 Akkermansia muciniphila gen. nov., sp. nov., a human intestinal mucin-degrading bacterium. Int J Syst Evol Microbiol 54, 1469–1476. [PubMed: 15388697]

Dewulf EM, Cani PD, Neyrinck AM, Possemiers S, Van Holle A, Muccioli GG, Deldicque L, Bindels LB, Pachikian BD, Sohet FM, Mignolet E, Francaux M, Larondelle Y, Delzenne NM, 2011 Inulin-type fructans with prebiotic properties counteract GPR43 overexpression and PPARgamma-related adipogenesis in the white adipose tissue of high-fat diet-fed mice. J Nutr Biochem 22, 712–722. [PubMed: 21115338]

Everard A, Lazarevic V, Gaia N, Johansson M, Stahlman M, Backhed F, Delzenne NM, Schrenzel J, Francois P, Cani PD, 2014 Microbiome of prebiotic-treated mice reveals novel targets involved in host response during obesity. ISME J 8, 2116–2130. [PubMed: 24694712]

Flint HJ, Scott KP, Duncan SH, Louis P, Forano E, 2012 Microbial degradation of complex carbohydrates in the gut. Gut Microbes 3, 289–306. [PubMed: 22572875]

Florowska A, Krygier K, Florowski T, Dluzewska E, 2016 Prebiotics as functional food ingredients preventing diet-related diseases. Food Funct 7, 2147–2155. [PubMed: 26961814]

Ganesh BP, Klopfleisch R, Loh G, Blaut M, 2013 Commensal Akkermansia muciniphila exacerbates gut inflammation in Salmonella Typhimurium-infected gnotobiotic mice. PLoS One 8, e74963. [PubMed: 24040367]

Hazlehurst JM, Woods C, Marjot T, Cobbold JF, Tomlinson JW, 2016 Non-alcoholic fatty liver disease and diabetes. Metabolism 65, 1096–1108. [PubMed: 26856933]

Hennig B, Ormsbee L, McClain CJ, Watkins BA, Blumberg B, Bachas LG, Sanderson W, Thompson C, Suk WA, 2012 Nutrition can modulate the toxicity of environmental pollutants: implications in risk assessment and human health. Environ Health Perspect 120, 771–774. [PubMed: 22357258]

Javadi L, Khoshbaten M, Safaiyan A, Ghavami M, Abbasi MM, Gargari BP, 2018 Pro- and prebiotic effects on oxidative stress and inflammatory markers in non-alcoholic fatty liver disease. Asia Pac J Clin Nutr 27, 1031–1039. [PubMed: 30272851]

Jensen TK, Timmermann AG, Rossing LI, Ried-Larsen M, Grontved A, Andersen LB, Dalgaard C, Hansen OH, Scheike T, Nielsen F, Grandjean P, 2014 Polychlorinated biphenyl exposure and glucose metabolism in 9-year-old Danish children. J Clin Endocrinol Metab 99, E2643–2651. [PubMed: 25093617]

Johnson JS, Spakowicz DJ, Hong BY, Petersen LM, Demkowicz P, Chen L, Leopold SR, Hanson BM, Agresta HO, Gerstein M, Sodergren E, Weinstock GM, 2019 Evaluation of 16S rRNA gene sequencing for species and strain-level microbiome analysis. Nat Commun 10, 5029. [PubMed: 31695033]

Keramida G, Hunter J, Peters AM, 2016 Hepatic glucose utilization in hepatic steatosis and obesity. Biosci Rep 36.

Knapp S, de Vos AF, Florquin S, Golenbock DT, van der Poll T, 2003 Lipopolysaccharide binding protein is an essential component of the innate immune response to Escherichia coli peritonitis in mice. Infect Immun 71, 6747–6753. [PubMed: 14638760]

Lagkouvardos I, Pukall R, Abt B, Foesel BU, Meier-Kolthoff JP, Kumar N, Bresciani A, Martinez I, Just S, Ziegler C, Brugiroux S, Garzetti D, Wenning M, Bui TP, Wang J, Hugenholtz F, Plugge CM, Peterson DA, Hornef MW, Baines JF, Smidt H, Walter J, Kristiansen K, Nielsen HB, Haller D, Overmann J, Stecher B, Clavel T, 2016 The Mouse Intestinal Bacterial Collection (miBC) provides host-specific insight into cultured diversity and functional potential of the gut microbiota. Nat Microbiol 1, 16131. [PubMed: 27670113]

Le Roy T, Llopis M, Lepage P, Bruneau A, Rabot S, Bevilacqua C, Martin P, Philippe C, Walker F, Bado A, Perlemuter G, Cassard-Doulcier AM, Gerard P, 2013 Intestinal microbiota determines development of non-alcoholic fatty liver disease in mice. Gut 62, 1787–1794. [PubMed: 23197411]

Mandal PK, 2005 Dioxin: a review of its environmental effects and its aryl hydrocarbon receptor biology. J Comp Physiol B 175, 221–230. [PubMed: 15900503]

Mensink MA, Frijlink HW, van der Voort Maarschalk K, Hinrichs WL, 2015 Inulin, a flexible oligosaccharide. II: Review of its pharmaceutical applications. Carbohydr Polym 134, 418–428. [PubMed: 26428143]

Mistry RH, Gu F, Schols HA, Verkade HJ, Tietge UJF, 2018 Effect of the prebiotic fiber inulin on cholesterol metabolism in wildtype mice. Sci Rep 8, 13238. [PubMed: 30185894]

Moos WH, Faller DV, Harpp DN, Kanara I, Pernokas J, Powers WR, Steliou K, 2016 Microbiota and Neurological Disorders: A Gut Feeling. Biores Open Access 5, 137–145. [PubMed: 27274912]

Perkins JT, Petriello MC, Newsome BJ, Hennig B, 2016 Polychlorinated biphenyls and links to cardiovascular disease. Environ Sci Pollut Res Int 23, 2160–2172. [PubMed: 25877901]

Petriello MC, Brandon JA, Hoffman J, Wang C, Tripathi H, Abdel-Latif A, Ye X, Li X, Yang L, Lee E, Soman S, Barney J, Wahlang B, Hennig B, Morris AJ, 2018 Dioxin-like PCB 126 Increases Systemic Inflammation and Accelerates Atherosclerosis in Lean LDL Receptor-Deficient Mice. Toxicol Sci 162, 548–558. [PubMed: 29216392]

Petriello MC, Hoffman JB, Sunkara M, Wahlang B, Perkins JT, Morris AJ, Hennig B, 2016 Dioxin-like pollutants increase hepatic flavin containing monooxygenase (FMO3) expression to promote synthesis of the pro-atherogenic nutrient biomarker trimethylamine N-oxide from dietary precursors. J Nutr Biochem 33, 145–153. [PubMed: 27155921]

Petriello MC, Hoffman JB, Vsevolozhskaya O, Morris AJ, Hennig B , 2018 Dioxin-like PCB 126 increases intestinal inflammation and disrupts gut microbiota and metabolic homeostasis. Environ Pollut 242, Part A, 1022–1032. [PubMed: 30373033]

Robles Alonso V, Guarner F, 2013 Linking the gut microbiota to human health. Br J Nutr 109 Suppl 2, S21–26. [PubMed: 23360877]

Salazar N, Dewulf EM, Neyrinck AM, Bindels LB, Cani PD, Mahillon J, de Vos WM, Thissen JP, Gueimonde M, de Los Reyes-Gavilan CG, Delzenne NM, 2015 Inulin-type fructans modulate intestinal Bifidobacterium species populations and decrease fecal short-chain fatty acids in obese women. Clin Nutr 34, 501–507. [PubMed: 24969566]

Sugatani J, Sadamitsu S, Wada T, Yamazaki Y, Ikari A, Miwa M, 2012 Effects of dietary inulin, statin, and their co-treatment on hyperlipidemia, hepatic steatosis and changes in drug-metabolizing enzymes in rats fed a high-fat and high-sucrose diet. Nutr Metab (Lond) 9, 23. [PubMed: 22452877]

Sugatani J, Wada T, Osabe M, Yamakawa K, Yoshinari K, Miwa M, 2006 Dietary inulin alleviates hepatic steatosis and xenobiotics-induced liver injury in rats fed a high-fat and high-sucrose diet: association with the suppression of hepatic cytochrome P450 and hepatocyte nuclear factor 4alpha expression. Drug Metab Dispos 34, 1677–1687. [PubMed: 16815962]

Tachon S, Zhou J, Keenan M, Martin R, Marco ML, 2013 The intestinal microbiota in aged mice is modulated by dietary resistant starch and correlated with improvements in host responses. FEMS Microbiol Ecol 83, 299–309. [PubMed: 22909308]

Tripathi A, Debelius J, Brenner DA, Karin M, Loomba R, Schnabl B, Knight R, 2018 The gut-liver axis and the intersection with the microbiome. Nat Rev Gastroenterol Hepatol 15, 397–411. [PubMed: 29748586]

Van Hul M, Geurts L, Plovier H, Druart C, Everard A, Stahlman M, Rhimi M, Chira K, Teissedre PL, Delzenne NM, Maguin E, Guilbot A, Brochot A, Gerard P, Backhed F, Cani PD, 2018 Reduced obesity, diabetes, and steatosis upon cinnamon and grape pomace are associated with changes in gut microbiota and markers of gut barrier. Am J Physiol Endocrinol Metab 314, E334–E352. [PubMed: 28874357]

Vandeputte D, Falony G, Vieira-Silva S, Wang J, Sailer M, Theis S, Verbeke K, Raes J, 2017 Prebiotic inulin-type fructans induce specific changes in the human gut microbiota. Gut 66, 1968–1974. [PubMed: 28213610]

Wahlang B, Barney J, Thompson B, Wang C, Hamad OM, Hoffman JB, Petriello MC, Morris AJ, Hennig B, 2017a Editor's Highlight: PCB126 Exposure Increases Risk for Peripheral Vascular Diseases in a Liver Injury Mouse Model. Toxicol Sci 160, 256–267. [PubMed: 28973532]

Wahlang B, Beier JI, Clair HB, Bellis-Jones HJ, Falkner KC, McClain CJ, Cave MC, 2013 Toxicant-associated steatohepatitis. Toxicol Pathol 41, 343–360. [PubMed: 23262638]

Wahlang B, Perkins JT, Petriello MC, Hoffman JB, Stromberg AJ, Hennig B, 2017b A Compromised Liver Alters Polychlorinated Biphenyl-Mediated Toxicity. Toxicology.

World Health Organization, 2016 WHO releases country estimates on air pollution exposure and health impact.

Zhang X, Zhao Y, Xu J, Xue Z, Zhang M, Pang X, Zhang X, Zhao L, 2015 Modulation of gut microbiota by berberine and metformin during the treatment of high-fat diet-induced obesity in rats. Sci Rep 5, 14405. [PubMed: 26396057]

- Inulin attenuated PCB 126 induced liver lipid accumulation and inflammation.
- Inulin decreased atherosclerotic lesion formation accelerated by PCB 126.
- Inulin normalized PCB 126 disturbed gut microbiota.

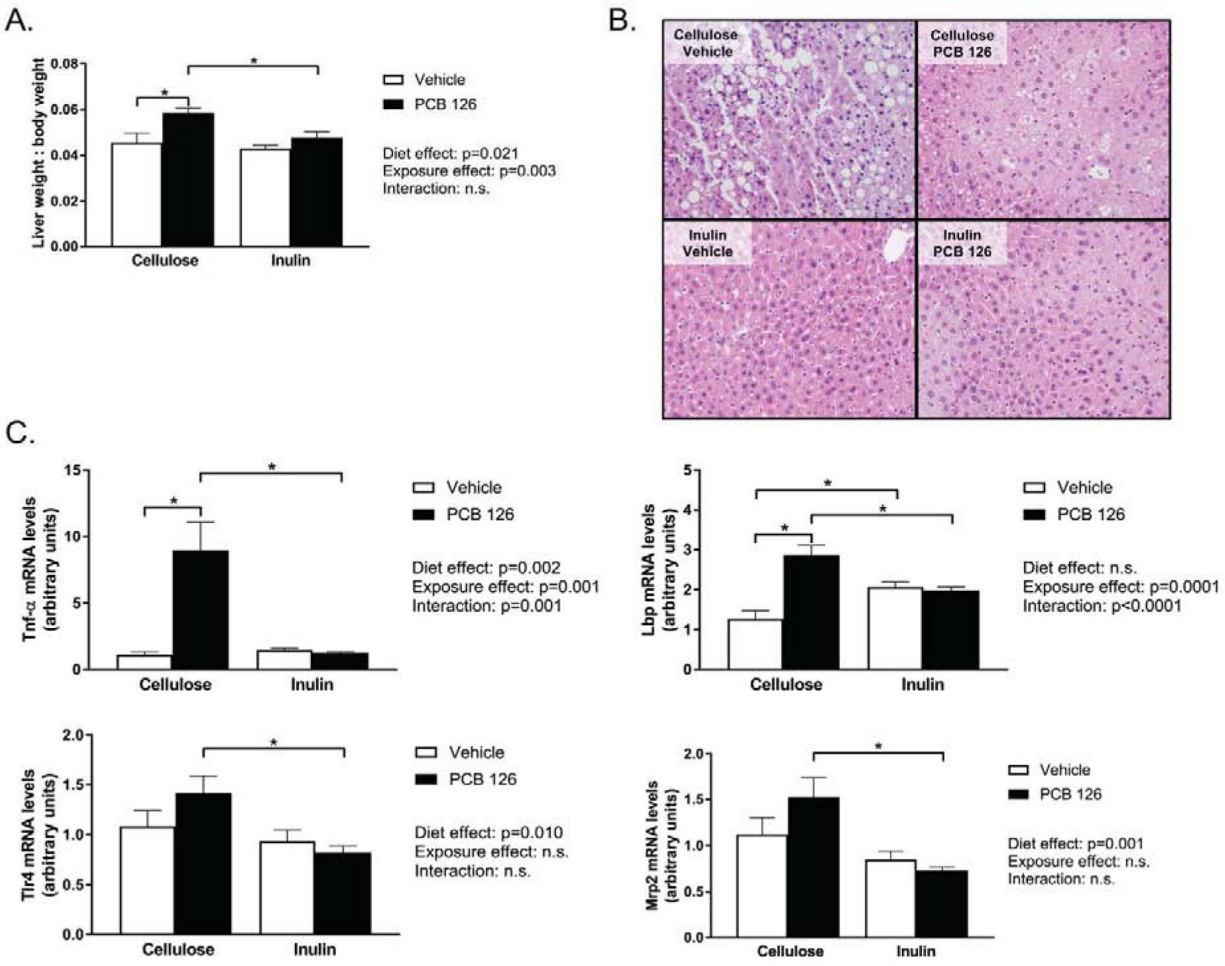

Figure 1. Inulin consumption reduces PCB-induced hepatic lipid accumulation.

Male *Ldlr*$^{-/-}$ mice were fed an atherogenic diet containing 8% cellulose or 8% inulin for 12 weeks and exposed to PCB 126 (1μmol/kg) or vehicle at weeks 2 and 4. **A.** Liver weight/ body weight ratio. PCB exposure increased liver weight in cellulose fed mice, which was attenuated by inulin feeding. **B.** Hematoxylin and eosin staining of hepatic tissue sections. Increases in microvescicular fat accumulation was evident in PCB exposed mice fed cellulose, which appeared to be attenuated by inulin consumption. Inulin feeding also had an overall effect of reducing macrovesicular fat accumulation. . **C.** mRNA quantification of hepatic markers of inflammation and xenobiotic detoxification. PCB exposure increased expression of tumor necrosis factor alpha (Tnfα) and lipopolysaccharide binding protein (Lbp), which was attenuated by inulin consumption. Toll like receptor 4 (Tlr4) and multidrug resistance protein (Mrp2) expression was lower in exposed inulin fed mice compared to exposed cellulose fed mice. Data are presented as mean ± S.E.M (n=10 per group). Statistical significance is denoted by * ($p<0.05$).

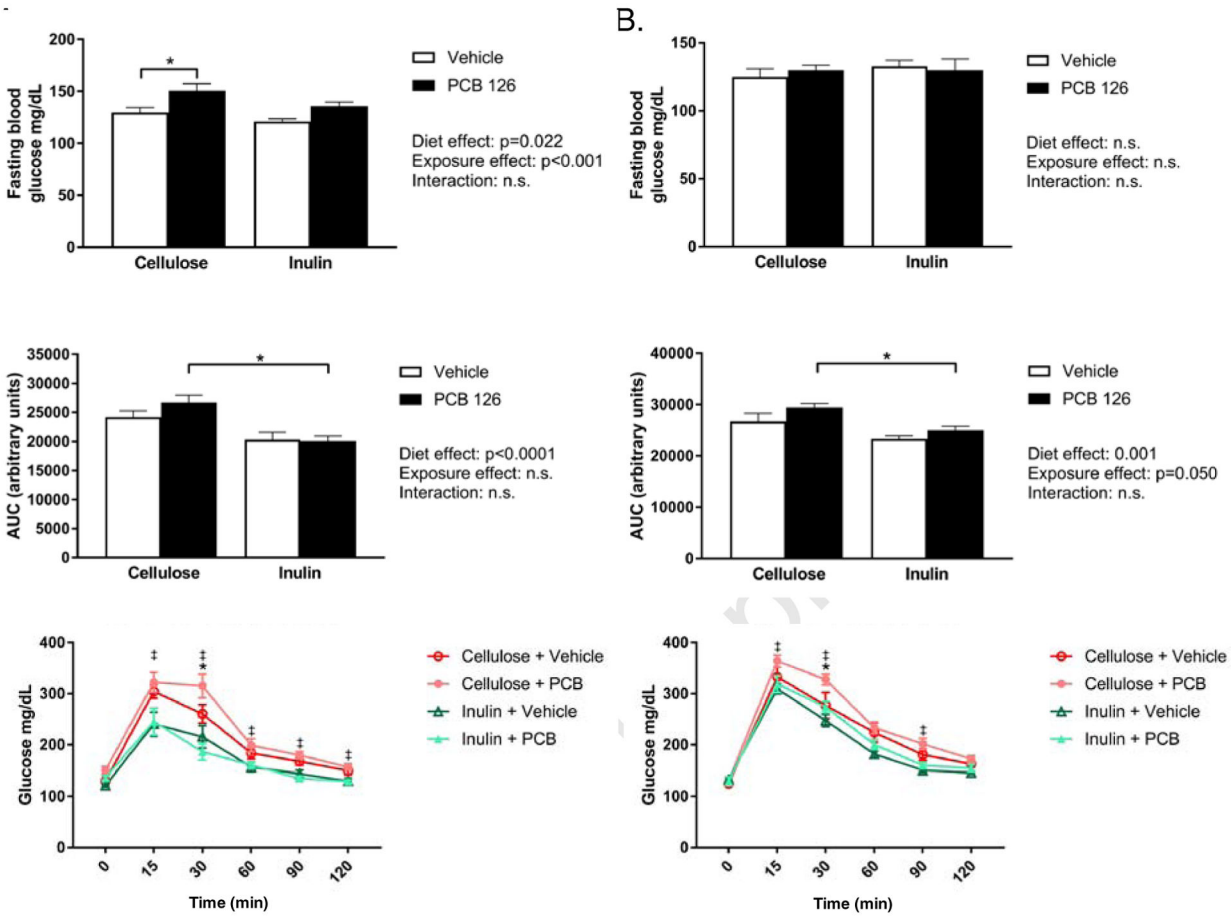

Figure 2. Inulin attenuates PCB-disruption in glucose tolerance.

Male *Ldlr*$^{-/-}$ mice were fed an atherogenic diet containing 8% cellulose or 8% inulin for 12 weeks and exposed to PCB 126 (1μmol/kg) or vehicle at weeks 2 and 4. **A.** Fasting blood glucose and glucose tolerance testing at week 5. PCB exposure increased fasting blood glucose levels in cellulose fed mice and not in inulin fed mice. Cellulose fed mice exposed to PCBs displayed a greater area under the curve (AUC) compared to exposed inulin fed mice. **B.** Fasting blood glucose and glucose tolerance testing at week 8. No differences were observed in fasting blood glucose. The effects of PCBs and diet on AUC remained significant at 8 weeks. Data are presented as mean ± S.E.M (n=10 per group). Statistical significance is denoted by * ($p<0.05$). For glucose curves, ‡ indicates a significant difference between “Cellulose + PCB” and “Inulin + PCB” and * indicates a significant difference between “Cellulose + Vehicle” and “Cellulose + PCB”.

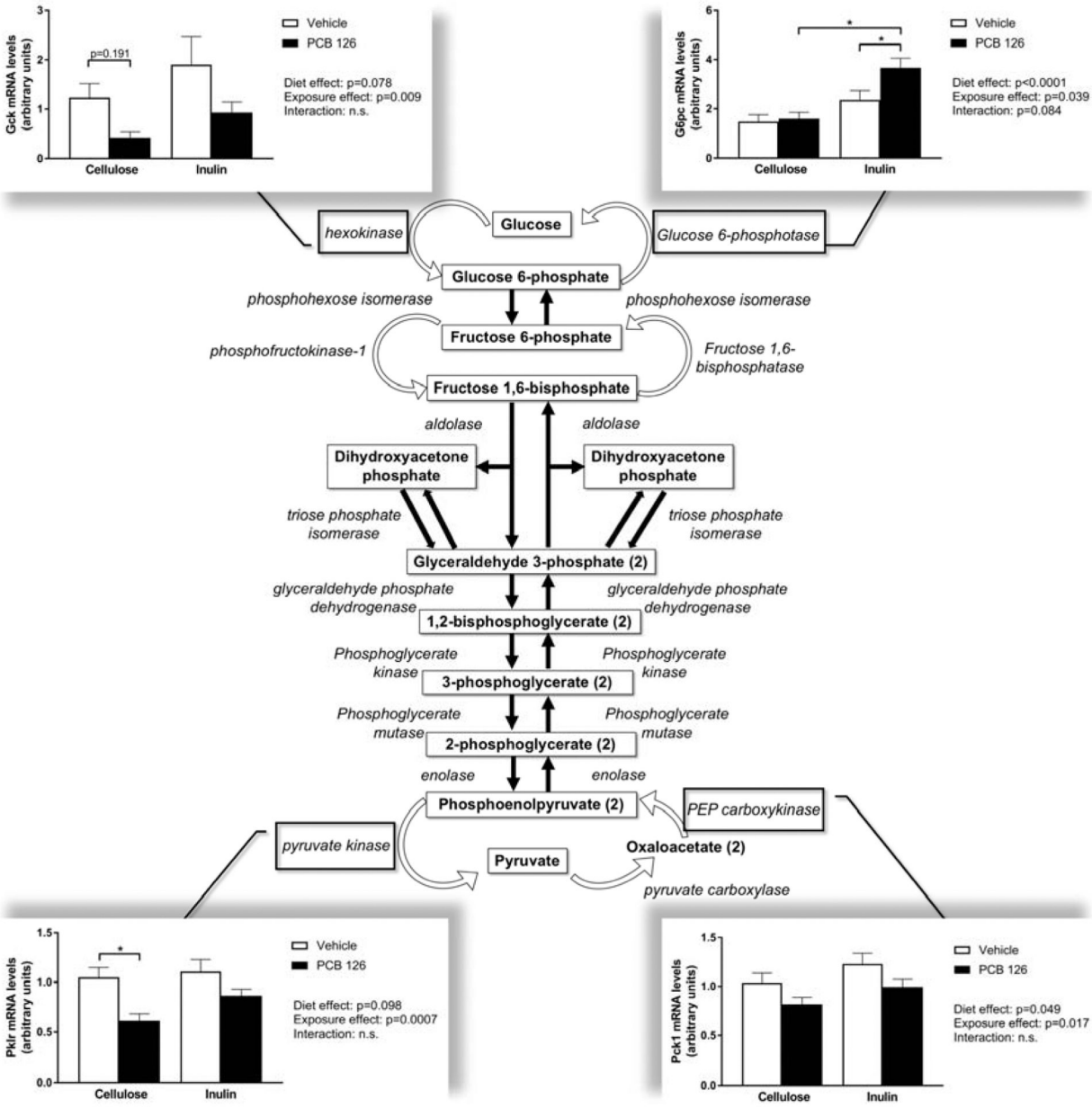

Figure 3. PCB disruption of glucose metabolism is attenuated by inulin.

Male *Ldlr*$^{-/-}$ mice were fed an atherogenic diet containing 8% cellulose or 8% inulin for 12 weeks and exposed to PCB 126 (1μmol/kg) or vehicle at weeks 2 and 4. Liver samples were collected at the conclusion of the study. mRNA units were determined using the relative quantification method (ΔΔCT), normalized to control values. 18S was used as the housekeeping gene for all hepatic gene expression quantifications. PCB exposure reduced expression of rate limiting glycolytic enzymes glucokinase/hexokinase (*Gck*) and pyruvate kinase (*Pklr*), which was not observed in inulin fed mice. Overall, inulin feeding increased gluconeogenic enzyme expression including PEP carboxykinase (Pck1) and glucose-6-phosphate (G6pc) irrespective of exposure. Data are presented as mean ± S.E.M (n=10 per group). Statistical significance is denoted by * ($p<0.05$).

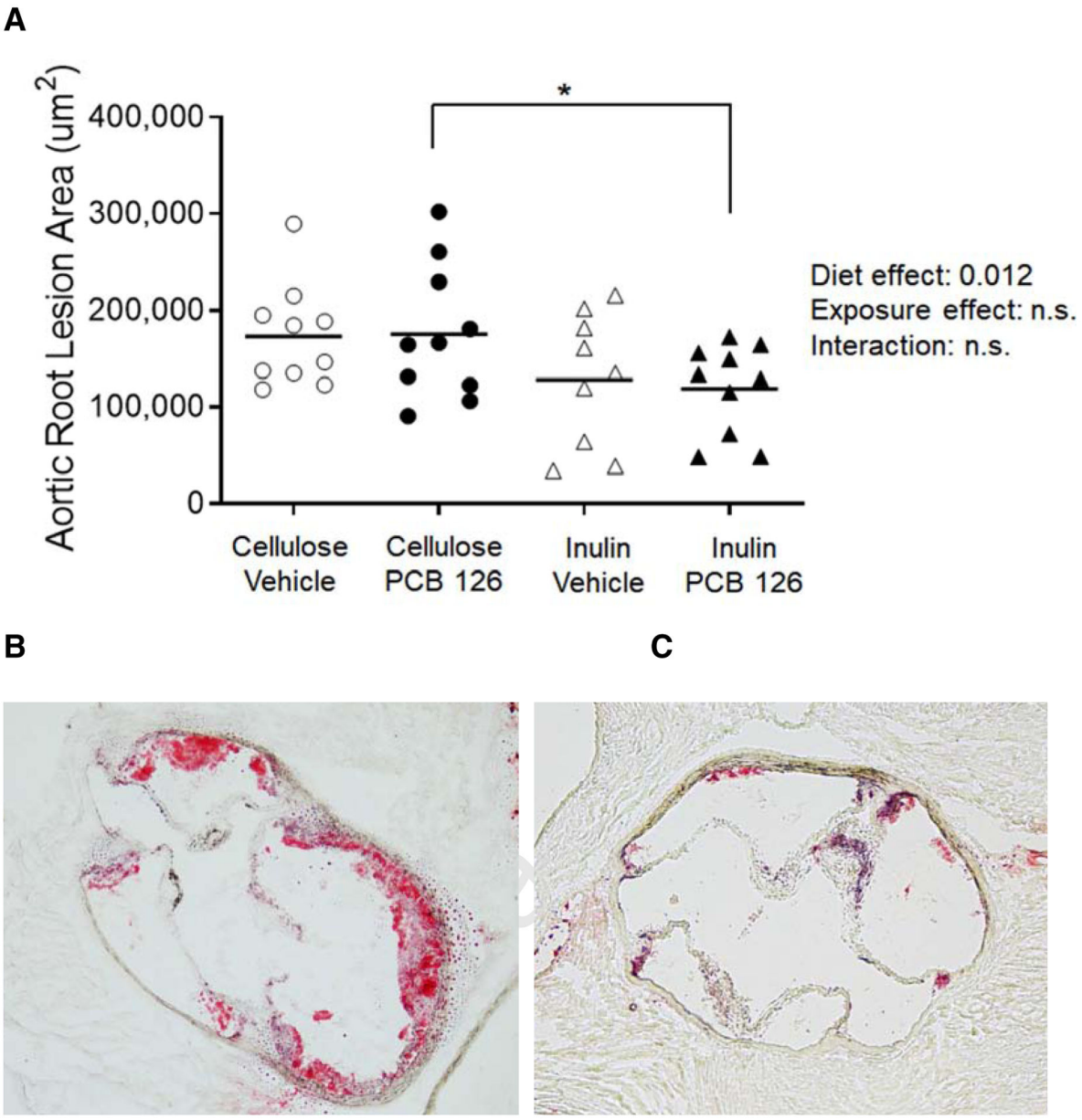

Figure 4. Inulin decreases aortic root lesion area in Ldlr deficient mice.

Male *Ldlr*$^{-/-}$ mice were fed a high cholesterol diet containing 8% cellulose or 8% inulin for 12 weeks and exposed to PCB 126 (1μmol/kg) or vehicle at weeks 2 and 4. A) Extent of atherosclerosis was determined by oil red-o staining of the aortic root. B and C) Representative cross section of the aortic roots from cellulose+PCB (B) and inulin+PCB (C) mice. Inulin significantly decreased lesion formation irrespective of treatment and mice fed the diet enriched with inulin and exposed to PCB 126 exhibited significantly decreased lesion formation compared to mice fed the control diet and exposed to PCB 126. (n=9–10 per group), Statistical significance is denoted by * ($p<0.05$).

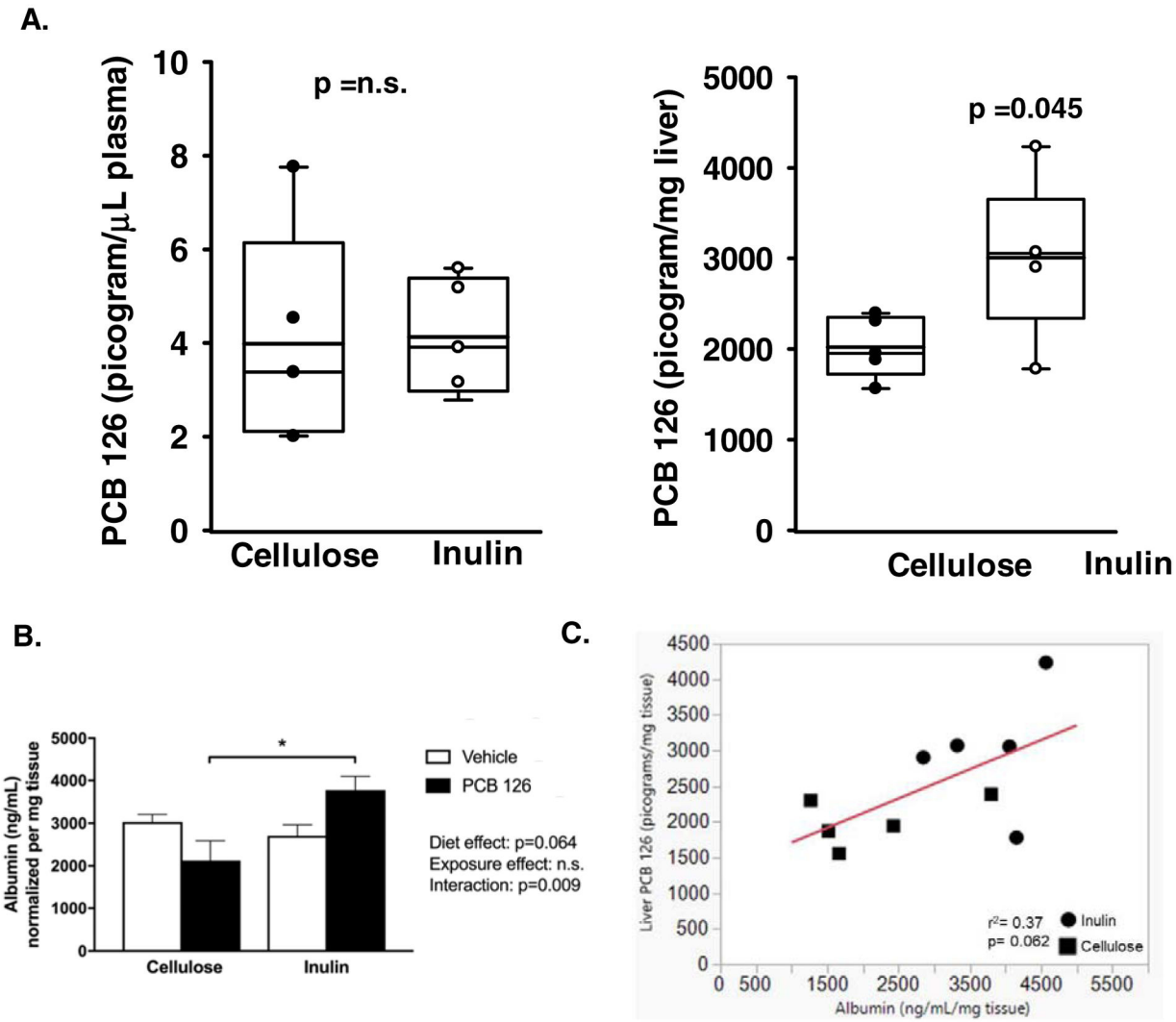

Figure 5. Inulin does not modulate circulating levels of PCB 126 but modulates hepatic levels of PCB 126 and albumin.

Male *Ldlr*$^{-/-}$ mice were fed a high cholesterol diet containing 8% cellulose or 8% inulin for 12 weeks and exposed to PCB 126 (1μmol/kg) or vehicle at weeks 2 and 4. A) Concentrations of PCB 126 were determined by GC-MS/MS in plasma and liver at the conclusion of the study. Inulin had no impact on circulating PCB 126 but increased hepatic levels (n=5 per group; p=0.045). No PCB 126 was observed in vehicle treated mice. B) Hepatic albumin concentrations (ng/mL/mg tissue) were quantified by ELISA. Overall, inulin significantly increases hepatic albumin levels and mice fed inulin and exposed to PCB 126 exhibited ~2-fold increase in albumin protein compared with exposed mice fed cellulose as the fiber source (n=4–5 per group). Statistical significance is denoted by * ($p<0.05$). C) A nearly significant positive association between hepatic albumin and hepatic PCB 126 levels were observed (p=0.062).

Environ Pollut. Author manuscript; available in PMC 2021 June 01.

Table 1

Phyla and genera differences in gut microbial populations shown in actual reads and relative abundance

	Cellulose + Vehicle		Cellulose + PCB 126		Inulin + Vehicle		Inulin + PCB 126	
Phyla	*Actual Reads*	*Relative Abundance(%)*	*Actual Reads*	*Relative Abundance (%)*	*Actual Reads*	*Relative Abundance (%)*	*Actual Reads*	*Relative Abundance (%)*
Actinobacteria$^{\#}$	17.8 ± 3.2	0.02 ± 0.004	32.7 ± 9.8	0.04 ± 0.01	604.0 ± 137.4*	0.74 ± 0.18*	1443.2 ±197.5*‡	1.94 ± 0.25*‡
Bacteroidetes$^{\#}$	12730.8 ± 2468.6	15.35 ± 2.72	10020.2 ± 1636.8	13.23 ± 2.15	28962.1 ± 1983.8*	36.97 ± 4.17*	15946.7 ± 1894.5‡	21.70 ± 2.59‡
Firmicutes$^{\#}$	28488.4 ± 2974.5	34.02 ± 1.99	22729.7 ± 1972.2	29.48 ± 2.31	20001.8 ± 2243.2	27.48 ± 3.49	24398.2 ± 2434.9	32.04 ± 1.92
Proteobacteria$^{\$@}$	2920.3 ± 706.1	3.47 ± 0.89	1364.4 ±246.8‡	1.80 ± 0.33‡	1599.3 ± 134.6	2.15 ± 0.24	1013.8 ±133.3	1.37 ± 0.18
Tenericutes$^{\#}$	83.0 ± 40.1	0.09 ± 0.04	137.9 ±37.5	0.19 ± 0.05	203.7 ± 48.0	0.27 ± 0.07	78.8 ± 23.2	0.10 ± 0.03
Verrucomicrobia$^{\$@}$	37404.8 ± 2784.3	46.59 ± 3.55	43083.4 ± 3849.8	54.95 ± 3.07	21070.8 ± 2235.6*	31.68 ± 3.91*	31417.9 ± 2044.9‡	41.79 ± 1.21‡
Genera	*Actual Reads*	*Relative Abundance(%)*	*Actual Reads*	*Relative Abundance (%)*	*Actual Reads*	*Relative Abundance (%)*	*Actual Reads*	*Relative Abundance (%)*
Bifidobacterium$^{\#}$	12.1 ± 3.0	0.02 ± 0.003	24.1 ± 9.7	0.03 ± 0.01	597.2 ± 136.7*	0.66 ± 0.18*	1432.5 ± 196.6*‡	1.92 ± 0.25*‡
Lactobacillus$^{\#}$	19.8 ± 6.7	0.03 ± 0.01	13.1 ± 4.8	0.02 ± 0.01	152.1 ± 41.9*	0.17 ± 0.06*	403.1 ± 95.9*‡	0.51 ± 0.09*‡
Lactococcus-	219.6 ± 42.7	0.27 ± 0.05	212.1 ± 72.4	0.26 ± 0.08	123.7 ± 19.5	0.17 ± 0.03	161.3 ± 31.3	0.23 ± 0.04
Turicibactef$^{\#}$	38.5 ± 10.4	0.05 ± 0.01	11.7 ± 3.0‡	0.01 ± 0.003‡	3.6 ± 0.8*	0.01 ± 0.001*	3.9 ± 1.3	0.005 ± 0.001
Clostridium$^{\$}$	18.4 ± 4.3	0.02 ± 0.004	19.6 ± 2.9	0.03 ± 0.004	4.2 ± 1.4*	0.01 ± 0.002*	2.5 ± 0.7*	0.004 ± 0.001*
Dehalobacterium$^{@}$	74.2 ± 8.8	0.09 ± 0.01	43.9 ± 7.7	0.06 ± 0.01	88.3 ± 23.2	0.10 ± 0.03	46.3 ± 7.9	0.06 ± 0.01
Coprococcus$^{\#}$	302.0 ± 38.0	0.36 ± 0.04	863.6 ± 234.4‡	1.09 ± 0.26‡	61.9 ± 21.0*	0.19 ± 0.03*	108.7 ± 23.5	0.14 ± 0.02
Dorea$^{\#}$	126.0 ±14.7	0.16 ± 0.02	41.2 ± 13.4‡	0.05 ± 0.02‡	21.3 ± 8.2*	0.03 ± 0.01*	16.4 ± 4.7*	0.02 ± 0.01*
[Ruminococcus]$^{\#}$	462.0 ± 58.0	0.55 ± 0.04	560.4 ± 35.1	0.72 ± 0.05	129.0 ± 16.3	0.22 ± 0.03	908.0 ± 193.5‡	1.28 ± 0.29‡
rc4–4$^{\#}$	1405.0 ± 409.1	1.66 ± 0.44	0.8 ± 0.5‡	0.001 ± 0.0004‡	211.0 ± 96.1*	0.23 ± 0.13*	249.0 ± 44.9*	0.33 ± 0.05*
Oscillospira$^{\$@}$	2755.2 ± 352.2	3.26 ± 0.25	1784.1 ± 214.2‡	2.27 ± 0.21‡	1251.0 ± 215.7*	1.64 ± 0.32*	1115.0 ± 118.4	1.53 ± 0.19

	Cellulose + Vehicle		Cellulose + PCB 126		Inulin + Vehicle		Inulin + PCB 126	
Ruminococcus $^{\#}$	727.4 ± 63.9	0.89 ± 0.06	861.8 ± 85.1	1.12 ± 0.10	545.6 ± 75.5	0.73 ± 0.12	340.8 ± 58.4 *	0.45 ± 0.07 *
Allobaculum $^{\#}$	5064.8 ± 1593.3	5.92 ±1.74	2007.5 ± 565.8	2.64 ± 0.77	12019.1 ± 2319.5 *	13.59 ± 3.05	14419.7 ± 1895.7 *	18.66 ± 1.52 *
Coprobacillus $^{\$}$	66.9 ± 14.2	0.08 ± 0.02	82.8 ± 16.1	0.11 ± 0.02	1.0 ± 0.5 *	0.01 ± 0.002 *	2.8 ± 1.0 *	0.004 ± 0.001 *
Sutterella $^{\#}$	772.2 ± 295.0	0.90 + 0.35	1092.1 ± 178.2	1.46 + 0.26	1585.3 ± 135.0 *	1.93 ± 0.25 *	993.7 ± 133.1	1.35 ± 0.17
Desulfovibrio $^{\#}$	2129.3± 811.1	2.55 + 1.01	6.2 ± 1.4 ‡	0.008 + 0.001 ‡	2.6 ± 0.8 *	0.004 ± 0.001 *	7.6 ± 3.6	0.01 ± 0.003
Akkermansia $^{\$@}$	37403.2 ± 2784.1	46.59 + 3.55	43081.5 ± 3849.6	54.94 + 3.07	21070.1 ± 2235.5 *	31.68 ± 3.91 *	31416.8 ± 2044.5 ‡	41.79 ± 1.21 ‡

Phyla and genera displayed are those with consistent quantifiable reads. Phyla classified as “other” were not included in the table.

*indicates a significant difference compared to cellulose diet of same treatment;

‡indicates a significant difference compared to vehicle of same diet (n=10).

$^{\$}$indicates a significant diet effect,

$^{@}$indicates a significant exposure,

$^{\#}$indicates a significant interaction between diet and exposure. Data analyzed by two-way ANOVA with post hoc comparisons of the means.